韓國鑛物學會誌 第 12 卷 第 2 號 (1999)
J. Miner. Soc. Korea, 12, 66-76 (1999)

Intergrowth of Biotite and Chlorite in an Amphibolitic Schist: Prograde or Retrograde Reaction?

각섬암에서 관찰된 흑운모와 녹니석의 협재 조직: 전진 또는 후퇴변성작용에 의한 것인가?

Jung Ho Ahn (안중호)* · Moonsup Cho (조문섭)**

*Department of Earth and Environmental Sciences, Chungbuk National University, Cheongju 361-763, Korea
(충북대학교 지구환경과학과)
**Department of Geological Sciences, Seoul National University, Seoul 151-742, Korea
(서울대학교 지질과학과)

ABSTRACT : Intergrowth texture of biotite and chlorite crystals within an amphibolitic schist of the northwestern Okchon metamorphic belt was investigated using back-scattered electron (BSE) imaging and high-resolution transmission electron microscopy (HRTEM). BSE images show that thin chlorite and biotite packets are mixed along (001) plane to result in intergrowth texture. In addition, rutile particles of submicron size occur exclusively at the boundaries between biotite and chlorite stacks. HRTEM investigation revealed that numerous low-angle grain boundaries are contained within chlorite crystals, and remnant biotite layers are closely associated with such boundaries, suggesting a possibility that chlorite layers were formed from biotite during retrograde metamorphic reaction. Such interpretation of the origin of intergrowth texture can be further supported by the occurrence rutile particles between the chlorite and biotite stacks: TiO_2 content of biotite is approximately 2 wt%, and that of chlorite usually lower than 0.2 wt%. Ti was apparently leached out during the alteration of biotite to precipitate rutile particles at the grain boundary area between biotite and chlorite stacks. Our observation suggests that such rutile particles could be an important indicator showing that the intergrowth texture of chlorite and biotite is originated by a retrograde metamorphism rather than by incomplete chlorite-to-biotite reaction during prograde metamorphism. Biotite crystals contain intercalated chlorite layers will result in somewhat high Mg and Al, and the use of such inhomogeneous biotite will result in imprecise geothermobarometric calculations.

요약 : 옥천변성대 북서부 지역에 산출하는 각섬암내의 흑운모/녹니석의 협재 조직에 관하여 후방산란 전자영상과 고분해능 투과전자현미경을 이용하여 조사하였다. 후방산란 전자영상 관찰에 의하면 매우 얇은 흑운모와 녹니석이 (001) 면을 따라서 혼합되는 협재 조직을 보여준다. 또한, 미세한 크기의 금홍석 입자들이 흑운모와 녹니석의 경계면에서만 발견된다. 고분해능 투과전자현미경 관찰에 의하면 많은 저각 경계들이 녹니석 결정내에 포함되어 있으며, 반응하지 않고 남아 있는 흑운모내의 Ti 성분이 녹니석에 포함되지 못하고 산화광물로 침전된 것으로 보인다. 이러한 결과는

금홍석 입자들이 흑운모/녹니석 협재조직이 전진변성작용시 불완전한 반응에 의한 것이 아니라 후퇴변성작용으로 인하여 생성되었음을 나타내는 유용한 지시광물로 사용될 수 있음을 제시한다. 특히, 녹니석을 포함하는 흑운모는 순수한 결정에 비하여 Mg와 Al의 함량이 다소 높게 나타나므로 이러한 흑운모를 이용한 온도와 압력의 계산은 부정확한 결과를 나타낼 수 있다.

INTRODUCTION

Metamorphic rocks commonly experience polymetamorphic events, and peak-metamorphic minerals could be altered to hydrous silicates to a variable extent. If early or prograde metamorphic minerals are preserved, they could provide us with critical evidences for deciphering the tectonic history of a given metamorphic region. Relict minerals indicative of an early metamorphic event may occur on a submicroscopic scale, and could be overlooked by routine examination using petrographic microscope.

The high-resolution transmission electron microscopy (HRTEM) is commonly used to reveal structural details below the unit-cell level of most minerals, and it has been widely used in mineralogical and crystallographic studies (cf. Allen, 1992; Veblen, 1992). However, recent studies using HRTEM have demonstrated the utility of such method as a powerful "high-resolution" petrographic microscope, and petrography can be done rigorously on a sub-micron scale (e.g., Lee *et al.*, 1984; Banfield *et al.*, 1989; Peacor, 1992). Sheet silicates are especially suitable for HRTEM investigation, because they are subject to various structural change and because layer structures of sheet silicates could be easily interpreted based on (001) lattice- fringe images.

Chlorite and biotite are common and important sheet silicates occurring under a wide range of geologic conditions. They are found in low- to medium-grade metamorphic rocks. Furthermore, chlorite could be formed as a secondary mineral that replaces primary ferromagnesisan silicates such as biotite. It is well known that chlorite structure consists of a talc-like layer and a brucite-like interlayer. As a result of the similarity between chlorite and biotite structures and their close association in altered rocks, there has been considerable interest in the chlorite-to-biotite reaction occurring during metamorphism and alteration. Direct solid-state transformation of biotite to chlorite has been suggested as the mechanism prevailing in various environments (Gilkes and Suddhiprakarn, 1979a, 1979b; Veblen and Ferry, 1983; Olives-Banos *et al.*, 1983; Olives-Banos and Amouric, 1984; Eggleton and Banfield, 1985; Kogure and Murakami, 1998).

Crystals composed of intergrown biotite and chlorite packets are commonly observed in metamorphic rocks. Biotite occurs in general at higher grade rocks than chlorite does. The intergrown texture could be originated by incomplete chlorite-to-biotite reaction during prograde metamorphism, or such texture could result from biotite-to-chlorite reaction during the episode of retrograde metamorphism. Both chlorite and biotite contain similar planar structural characteristics, and thus they tend to form intergrown stacks along the (001) plane. Therefore, the origin of such intergrown texture is very difficult to distinguish without detailed microstructural data.

In the present study, crystals constituted with intergrown chlorite and biotite from an amphibolitic schist were examined with back-scattered electron (BSE) imaging and HRTEM. Detailed investigation of such crystals may provide some clues for unravelling metamorphic history. The purposes of this study are to present microstructures of chlorite and biotite and to reveal the origin of chlorite-biotite intergrowth. We also report the structural defects in chlorite and biotite, structural variations, and other features on a few angstrom scale that are important for interpreting the P-T path of the Ogcheon metamorphic belt. This study complements our previous investigations on the structural defect in hornblende (Ahn and Cho, 1996, 1998).

EXPERIMENTAL METHODS

The amphibolitic schists investigated in this study are collected from the Chungju area, northwestern part of the Okchon metamorphic belt (Fig. 1). The specimen is identical with M416 of Min (1996), who reported a K-Ar hornblende age of 675±30 Ma. Ahn and Cho (1996, 1998) investigated the hornblende of the schists using HRTEM and found that hornblende crystals that appear unaltered and optically homogeneous contain various structural defects. Geological and petrological outlines of the Chungju area are available in Min and Cho (1998).

Polished thin sections oriented approximately perpendicular to the foliation and lineation, if any, in order to enhance the probability to find chlorite and biotite crystals cut approximately perpendicular to (001). Chemical analysis and BSE imaging were performed using a CAMECA SX-51 electron probe microanalyzer.

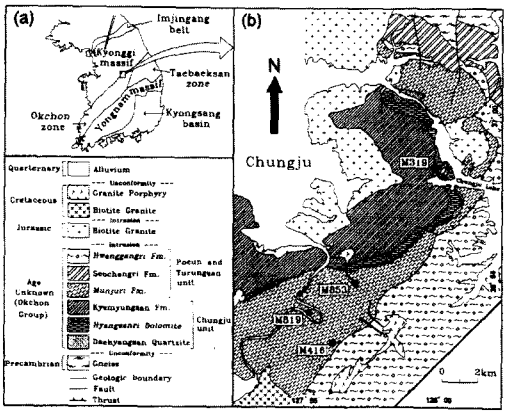

Fig. 1. Geological map showing the study area and the sample locations (adopted from Min and Cho, 1998).

Selected areas for the TEM observation were covered by 3-mm copper grids using epoxy glue, and detached from the specimen for ion-milling. Ion-milled specimens were investigated using a JEOL JEM-4000EX transmission electron microscope with a top-entry stage having tilting angles of ±15°, spherical aberration coefficient (C_s) of 1.0 mm, and structure resolution of 1.7 Å (Smith *et al.*, 1986). A 40-μm objective aperture and a 150-μm condenser aperture were used for the HRTEM imaging. Imaging of the specimens was performed with (001) of chlorite and biotite parallel to the electron beam. (001) lattice-fringe images were obtained from sheet silicates, and both sheet silicates were characterized by their (001) interplanar spacings.

RESULTS

BSE Image Observation

BSE imaging is very useful in characterizing

mineral zoning and intergrowth occurring below the resolution of petrographic microscope, because the mineral of high average atomic number produce more back-scattered electrons than the material of lower average atomic number to result in different contrast difference. BSE images of sheet silicates show two distinct contrast; the areas with darker contrast corresponds to chlorite, and the areas with brighter contrast is biotite (Fig. 2). BSE images of biotite and chlorite show that crystals they are intimately intergrown each other. The amount of intergrown sheet silicates varies from crystal to crystal. The intergrown materials are parallel to (001) of the host crystals, and their thickness is mostly of submicron scale.

Small particles showing very bright contrast are commonly observed with intergrown sheet silicates (Fig. 2). The thickness of such

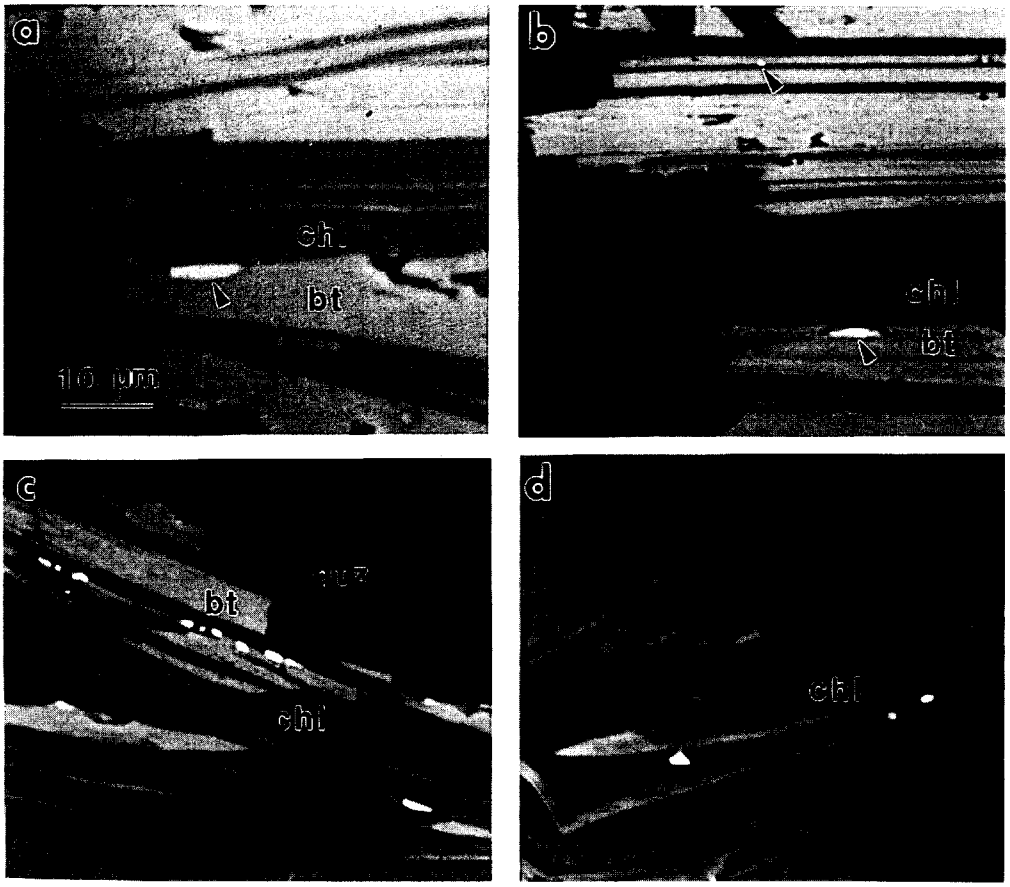

Fig. 2. BSE images showing the intergrowth texture of biotite and chlorite. The areas with darker contrast corresponds to chlorite, and the areas with brighter contrast is biotite. Submicron-size rutile particles showing very bright contrast are commonly observed at the boundaries between biotite and chlorite stacks.

particles is less than 1 μm that is much smaller than the electron beam size. Energy-dispersive spectroscopic (EDS) analyses of the area containing the particles result in excessive Ti content without the change of peaks from other elements, indicating the particles are titanium oxide. The occurrence of the TiO_2 particles within the metamorphic rock at a relatively high temperature excludes the possibility of them being other polymorphic minerals, such as anatase and brookite, and the particles are apparently rutile (Gribb and Banfield, 1984). Most rutile particles characteristically occur at the interface between biotite and chlorite packets. EPMA analyses show that TiO_2 content of biotite and chlorite is approximately 2 and 0.2 wt%, respectively (Table 1). Some chlorites showing significant amount of K exhibit relatively high amount of Ti, indicating the possible intergrowth of biotite

Table 1. Representative electron microprobe analyses of biotite and chlorite.

Oxides	biotite(1)	biotite(2)	chlorite(1)	chlorite(2)
SiO_2	36.65	36.91	26.94	27.36
Al_2O_3	16.36	15.58	20.59	20.71
MgO	12.25	14.28	22.50	21.43
FeO	16.16	15.96	16.25	16.98
MnO	0.28	0.22	0.37	0.22
TiO_2	1.88	1.94	0.12	0.26
K_2O	8.53	8.42	0.13	0.77
Na_2O	0.16	0.21	0.00	0.00
CaO	0.01	0.04	0.00	0.02
Total	94.28 wt%	94.88 wt%	86.91 wt%	87.74 wt%
	Ions per formula unit			
	biotite(1)	biotite(2)	chlorite(1)	chlorite(2)
Si	2.77	2.81	2.73	2.76
Al(IV)	1.23	1.19	1.27	1.24
ΣTet.	4.00	4.00	4.00	4.00
Al(VI)	0.23	0.21	1.19	1.26
Mg	1.60	1.62	3.40	3.23
Fe	1.02	1.01	1.38	1.43
Mn	0.02	0.01	0.03	0.02
Ti	0.11	0.11	0.01	0.02
ΣOct.	2.98	2.96	6.01	5.96
K	0.82	0.82	0.01	0.10
Na	0.02	0.03	0.00	0.00
Ca	0.00	0.00	0.00	0.00
ΣInt.	0.84	0.85		

* Total Fe reported as FeO.

** Biotite and chlorite formulae normalized to $O_{10}(OH)_2$ and $O_{10}(OH)_8$, respectively.

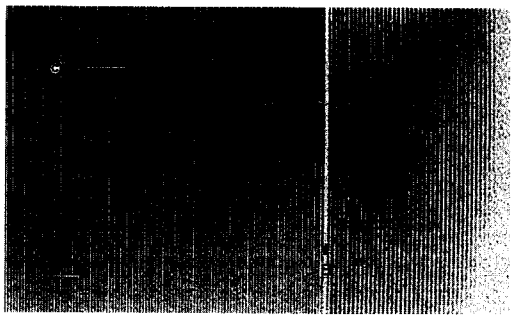

Fig. 3. HRTEM image showing the intergrown biotite (bt) and chlorite (chl) that are parallel along (001). An extra brucite-like layer (B), which is approximately 5 Å thick, occurs at the biotite-chlorite interface.

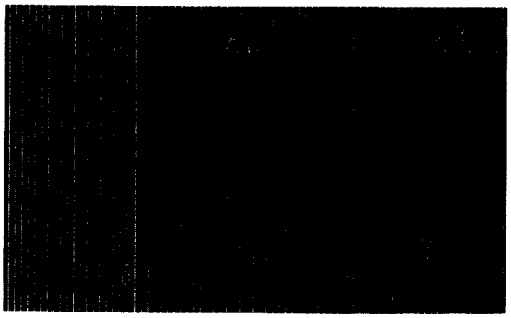

Fig. 4. HRTEM image showing extra brucite-like layers (B) that are intergrown within biotite crystals. Insertion of brucite-like layer at the interlayer of biotite results in a chlorite structure.

Fig. 5. HRTEM image showing numerous planar defects that commonly divide the chlorite grain into layers of packets. The (001) planes on either side are not parallel but inclined by few degrees to each other, and isolated single or several layers are intercalated within the chlorite crystal.

layers below electron microprobe resolution.

HRTEM Observation

HRTEM observations show that the (001) planes of intergrown biotite and chlorite are parallel (Fig. 3). Their boundaries are parallel along (001) of both minerals, and two sheet silicates are distinguishable by the difference in interplanar spacings. Fig. 3 shows an extra brucite-like layer, which is approximately 5 Å thick, at the biotite-chlorite interface, indicating the possibility of biotite-to-chlorite reaction. Extra brucite-like layers are frequently observed within biotite crystals (Fig. 4). Insertion of brucite-like layer at the interlayer of biotite

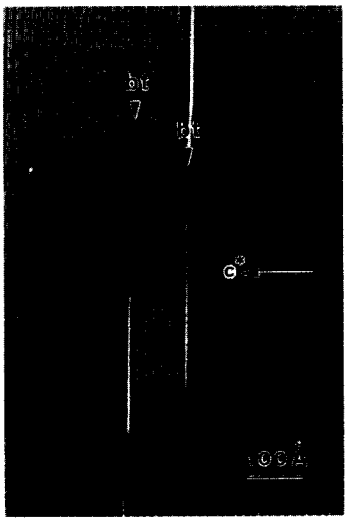

Fig. 6. HRTEM image showing the association of unreacted biotite layers with low-angle grain boundaries. Isolated biotite layers terminate at the low-angle grain boundaries area.

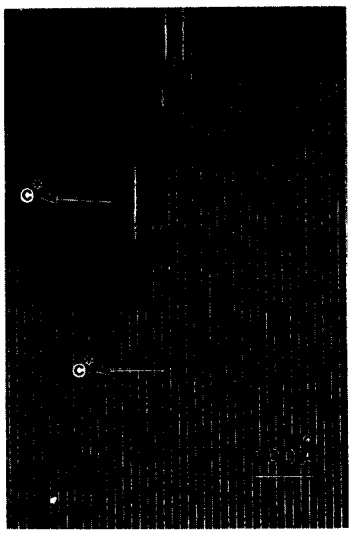

Fig. 7. HRTEM image showing low-angle grain boundaries that are contained within a single crystal. The presence of boundaries causes slight misorientation of chlorite layers.

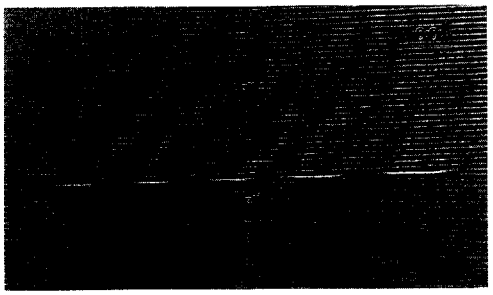

Fig. 8. HRTEM image showing periodic rows of triangular regions surrounded by two (001) chlorite planes. Chlorite layers become subparallel at the area where the low-angle grain boundaries terminate.

results in a chlorite structure (Veblen and Ferry, 1983).

Various low-angle grain boundaries are observed within chlorite crystals. Fig. 5 shows a (001) lattice-fringe image of chlorite. Planar defects commonly divide the chlorite grain into packets of layers several hundreds angstrom thick. The (001) planes on either side of packets are not parallel but inclined by several degrees to each other, and such planar defects constitute low-angle grain boundaries. They are initiated or terminated in a crystal, suggesting they are not formed by coalescence of two separate crystals growing independently (Kogure and Murakami, 1998). The boundaries consist of the (001) interface of a chlorite layer at one side and terminating chlorite layers at the other, so that the grain boundary involves a series of misorientation of few degrees. Furthermore, isolated single or several biotite layers are intercalated within the chlorite crystal (Fig. 5). Three and five biotite layers transit to chlorite layers at the bottom of the area of Fig. 5, indicating a possibility that the intercalated biotite layers are the

remnant biotite layers survived retrogressive reaction. The association of remnant biotite layers with low-angle grain boundaries within chlorite crystals supports a possibility that low-angle grain boundaries within chlorite crystals may have caused by the biotite-to-chlorite alteration.

The association of unreacted biotite layers with grain boundaries can be found in Fig. 6; isolated biotite layers remain in the chlorite crystal, and biotite layers terminate at the low-angle grain boundaries area. Chlorite layers on both sides of the boundaries are slightly misoriented by less than 1°. Low-angle grain boundaries are contained within a single crystal (Fig. 7), and the presence of boundaries causes slight misorientation of chlorite layers. The chlorite layers away from the boundary are perfectly parallel, indicating that the low-angle grain boundaries are not formed as a result of incorporation of separate crystals during crystal growth.

Fig. 8 shows periodic rows of triangular regions surrounded by two (001) chlorite planes and the edge terminating layer along the boundaries are formed along low-angle grain boundaries. Chlorite layers become subparallel at the area where the low-angle grain boundaries terminate. However, the chlorite layers on both sides of the boundaries differ in their orientations by few degrees.

DISCUSSION

Origin of the Intergrowth of Chlorite and Biotite

The rutile particles does not occur within biotite crystals that show higher TiO_2 content compared to chlorite (Table 1), suggesting that higher TiO_2 in biotite is not caused by inclusion of rutile particles within biotite. The rutile particles are exclusively found at the grain boundaries between biotite and chlorite (Fig. 2). Such occurrence of rutile particles indicates that they apparently formed during the biotite- to-chlorite alteration. Furthermore, higher amount of TiO_2 in biotite (Abrecht and Hewitt, 1988) than in chlorite also suggests that Ti was leached out during the formation chlorite from biotite; TiO_2 content of biotite is approximately 2 wt%, and that of chlorite usually lower than 0.2 wt%. Such analytical data indicate that Ti was leached out from biotite during decomposition and was not incorporated within chlorite structure. Released Ti was mostly oxidized to form rutile at the grain boundary area between biotite and chlorite.

The occurrence of rutile particles is direct evidence that the intergrown texture of biotite and chlorite is produced by retrogressive reaction of biotite. HRTEM images also show intergrown brucite-like layers within biotite structure (Figs. 3 and 4), and futhermore numerous low-angle grain boundaries associated with remnant biotite layers within chlorite crystals suggest the occurrence of biotite-to-chlorite reaction (Figs. 5 and 6). Numerous remnant biotite layers and grain boundaries within chlorite indicate that chlorite formed from biotite during retrograde metamorphism is not fully reequilibrated. It is well known that vermiculite or kaolinite commonly replace biotite layers during weathering (Eggleton and Banfield, 1985; Ahn and Peacor, 1987; Banfield and Eggleton, 1988), and the possibility of formation of chlorite by weathering process could be excluded.

The retrograde reaction of biotite to chlorite occurring in the study area is

compatible with the P-T history of north-western Ogcheon metamorphic belt. Min (1996) and Min and Cho (1998) reported that the Munjuri Formation near Chungju has experienced a peak metamorphism at 5-8 kbar and 520-590°C and subsequently a retrograde metamorphism at 1-3 kbar and 350-500°C. Hornblende-plagioclase pairs of sample M853 near the investigated specimen produced a temperature estimate of 590±5°C (Min and Cho, 1998), attesting to the equilibration of the rock during the peak metamorphism. However, subsequent retrograde metamorphism has promoted the biotite-to-chlorite reaction to result in chlorite and biotite intergrowth revealed in this study. The incomplete retrograde reaction of biotite to chlorite and production of intergrowth texture can be attributed to the sluggish mineral reaction at a relatively low temperature.

Implications for the Application to Biotite-bearing Geothermobarometry

Phase equilibria involving biotite have been widely used for the geothermobarometry in a variety of plutonic and metamorphic rocks (e.g., Ganguly and Saxena, 1984; Graham and Powell, 1984; Indares and Martignole, 1985; Berman, 1990; Hoisch, 1991). The partitioning of Fe and Mg between coexisting biotite and garnet has been extensively used as a geothermometer (e.g., Ferry and Spear, 1978; Ganguly and Saxena, 1984; Indares and Martignole, 1985; Berman, 1990). Geother-mobarometric calculations commonly assume that structures and chemistries of biotite are not affected by post-peak metamorphism. However, intergrowth of chlorite could occur in such a fine scale that electron microprobe analyses may not represent the true compositions of biotite. The analytical data of biotite and chlorite from the sample show significantly different Mg:Fe ratio; chlorite is highly enriched with Mg compared to biotite. Hence, the biotite containing intercalated chlorite layers would result in high Mg:Fe ratio, and the use of such biotite for geothermobarometry should result in incorrect estimations of temperature and pressure.

Micro-scale intergrowth of aluminous sheet silicates such as chlorite will result in excess Al in the analysis of biotite. In addition, differential partitioning of Mg and Fe between biotite and the intergrown chlorite may contribute to the uncertainty in Fe/Mg ratios of biotite, and consequently in P-T estimates. For example, the substitution of Al for Si in tetrahedral sites of biotite varies as a function of pressure and temperature (Indares and Martignole, 1985). Thus, calculations of temperature and pressure could be flawed by the overestimation of Mg and Al in biotite containing chlorite layers.

CONCLUSIONS

Thin chlorite and biotite packets are mixed along (001) plane to result in intergrowth of both sheet silicates. BSE images show that tiny rutile particles occur exclusively at the boundaries between biotite and chlorite stacks. HRTEM images show that numerous low-angle grain boundaries are contained within chlorite crystals, and remnant biotite layers are closely associated with such boundaries, suggesting that chlorite layers were formed from biotite during retrograde metamorphic reaction. The occurrence of rutile particles between the chlorite and biotite stacks supports the origin

of retrograde metamorphic reaction; TiO_2 content of biotite is approximately 2 wt%, and that of chlorite is usually lower than 0.2 wt%, and higher TiO_2 in biotite than in chlorite also suggests that most was Ti leached out from biotite was not incorporated within chlorite structure and oxidized to form rutile at the grain boundary area between biotite and chlorite. Our observations suggest that rutile particles occurring between the biotite and chlorite stacks could be important indicator that intergrowth texture of chlorite and biotite is of retrograde metamorphic origin rather that incomplete reaction of chlorite-to-biotite reaction during prograde metamorphic reaction. The formation of chlorite from biotite by retrograde reaction is consistent with the P-T history of northwestern Okchon metamorphic belt (Min, 1996; Min and Cho, 1998). In addition, biotite crystals containing intercalated chlorite layers will result in somewhat higher Mg and Al contents in the biotite analysis, producing imprecise result in geothermobarometric calculations.

ACKNOWLEDGMENTS

Electron microscopy was carried out at the Facility for High Resolution Electron Microscopy at Arizona State University with the kind help of Prof. P. R. Buseck. We thank Kyoungwon Min for helping us in many ways to complete this study. We also thank Dr. Jung Hoo Lee for Valuable comments and corrections. This study was funded by the project BSRI-97-5404 provided by the Ministry of Education, Korea.

REFERENCES

Abrecht, J. and Hewitt, D. A. (1988) Experimental evidence on the substitution of Ti in biotite. Amer. Mineral., 73, 1275-1284.

Ahn, J. H. and Cho, M. (1996) High-resolution electron microscopy of structural defects in hornblendes of Ogcheon amphibolites. J. Geol. Soc. Korea, 32, 334-344.

Ahn, J. H. and Cho, M. (1998) Sub-microscopic alteration of hornblende in the amphibolitic schists, northwestern Okchon metamorphic belt. Geoscience Journal, 2, 165-174.

Ahn, J. H. and Peacor, D. R. (1987) Kaolinitization of biotite: TEM data and implications for an alteration mechanism. Amer. Mineral., 72, 353-356.

Allen, F. M. (1992) Mineral definition by HRTEM: problems and opportunities. Rev. Mineral., 27, 288-333.

Banfield, J. B. and Eggleton, R. A. (1988) Transmission electron microscope study of biotite weathering. Clays Clay Miner., 36, 47-60.

Banfield, J. F., Karabinos, P. and Veblen, D. R. (1989) Transmission electron microscopy of chloritoid: intergrowth with sheet silicates and reaction mechanisms. Amer. Mineral., 74, 549-564.

Berman, R. G. (1990) Mixing properties of Ca-Mg-Fe-Mn garnets. Amer. Mineral., 75, 328-344.

Eggleton, R. A. and Banfield, J. F. (1985) The alteration of granitic biotite to chlorite. Amer. Mineral., 70, 902-910.

Ferry, J. M. and Spear, F. S. (1978) Experimental calibration of the partitioning of Fe and Mg between biotite and garnet. Contrib. Mineral. Petrol., 66, 113-117.

Ganguly, J. and Saxena, S. K. (1984) Mixing properties of aluminosilicates garnets: constraints from natural and experimental data, and applications to geothermobarometry. Amer. Mineral., 69, 88-97.

Gilkes, R. J. and Suddhiprakarn, A. (1979a) Biotite alteration in deeply weathered granite. I. morphological, mineralogical, and chemical properties. Clays Clay Miner., 27, 349-360.

Gilkes, R. J. and Suddhiprakarn, A. (1979b) Biotite alteration in deeply weathered granite. II. the oriented growth of secondary minerals. Clays Clay Miner., 27, 361-367.

Graham, C. M. and Powell, R. (1984) A garnet-hornblende geothermometer and application to the Pelona schist, southern California. J. Metamor. Geol., 2, 13-32.

Gribb, A. A. and Banfield, J. F. (1997) Particle size effects on transformation kinetics and phase stability in nanocrystalline TiO_2. Amer. Mineral., 82, 717-728.

Hoisch, T. D. (1991) Equilibria within the mineral assemblage quartz muscovite biotite garnet plagioclase, and implications for the mixing properties of octahedrally-coordinated cations in muscovite and biotite. Contrib. Mineral. Petrol., 108, 43-54.

Indares, A. and Martignole, J. (1985) Biotite-garnet geothermometry in the granulite facies: the influence of Ti and Al in biotite. Ameri. Mineral., 70, 272-278.

Kogure, T. and Murakami, T. (1998) Structure and formation mechanism of low-angle boundaries in chlorite. Amer. Mineral., 83, 358-364.

Lee, J. H., Peacor, D. R., Lewis, D. D. and Wintsch, R. P. (1984) Chlorite-illite/muscovite interlayered and interstratified crystals: Contrib. Mineral. Petrol., 88, 372-385.

Min, K. (1996) Metamorphism, thermochronology and P-T-t path of pelitic and mafic schists in the Chungju area, northwestern Ogcheon metamorphic belt, Korea. M.S. thesis, Seoul National University, Seoul, 87 p.

Min, K. and Cho. M. (1998) Metamorphic evolution of the northwestern Ogcheon metamorphic belt, South Korea. Lithos, 43, 31-51.

Olives Banos, J., Amouric, M., De Fouquet, C. and Baronnet, A. (1983) Interlayering and interlayer slip in biotite as seen by HRTEM. Amer. Mineral., 69, 754-758.

Olives Banos, J. and Amouric, M. (1984) Biotite chloritization by interplanar brucitization as een by HRTEM. Amer. Mineral., 69, 869-871.

Peacor, D. R. (1992) Diagenesis and low-grade metamorphism of shales and slates. Rev. Mineral., 27, 335-380.

Smith, D. J., Barry, J. C., Bursill, L. A., Petford, A. K. and Wheatley, J. C. (1986) Atomic resolution imaging of crystalline defects and surfaces. JEOL News, 24E, 2-6.

Veblen, D. R. (1992) Electron microscopy applied to nonstoichiometry, polysomatism, and replacement reactions in minerals. Rev. Mineral., 27, 181-229.

Veblen, D. R. and Ferry, J. M. (1983) A TEM study of the biotite-chlorite reaction and comparison with petrologic observations. Amer. Mineral., 68, 1160-1168.

1999년 6월 15일 원고접수, 12월 10일 게재승인.